Supplementary Figure 1

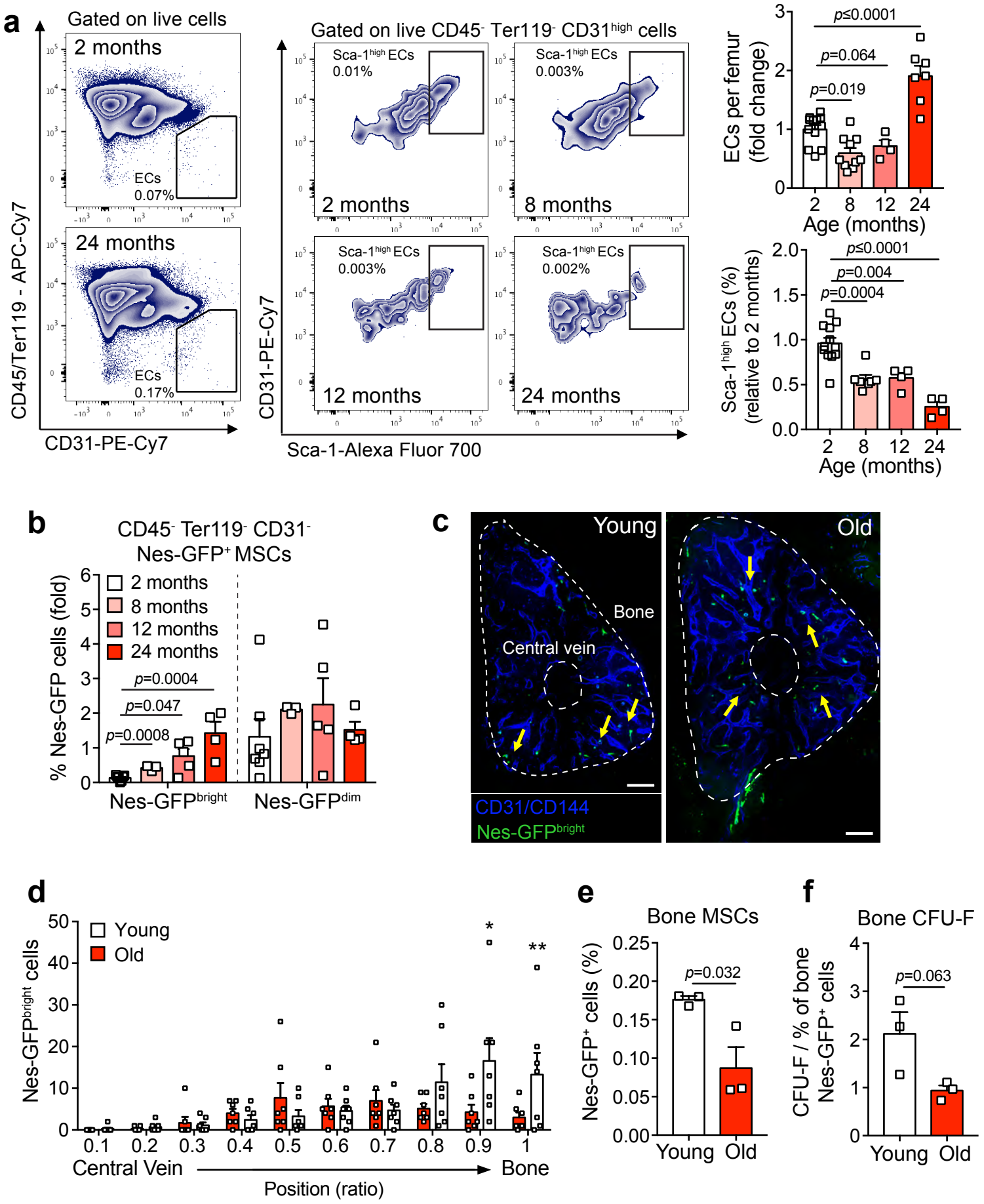

Supplementary Figure 1. Aging expands ECs and MSCs in the bone marrow. **(a)** Left and middle, gating strategy for flow cytometric analysis of EC populations. Right, absolute number of total ECs ($CD31^{high}$ $Sca\text{-}1^{+}$) at 2 (n=12), 8 (n=10), 12 (n=4) and 24 (n=7) months of age and arteriolar ECs ($CD31^{+}$ $Sca\text{-}1^{high}$) at 2 (n=12), 8 (n=7), 12 (n=4) and 24 (n=4) months of age. **(b)** Frequency of $CD45^{-}$ $Ter119^{-}$ $CD31^{-}$ $Nestin\text{-}GFP^{bright}$ and $Nestin\text{-}GFP^{dim}$ cells in *Nestin-GFP* mice at 2 (n=7), 8 (n=3), 12 (n=5) and 24 (n=4) months of age. **(c)** Confocal z stack montage projections of tibiae cross section from young and old *Nestin-GFP* mice stained for $CD31^{+}$/$CD144^{+}$ double positive vasculature, arrowhead marks Nestin-GFP ensheathed arterioles. The scale bar, 100 μm. Three independent experiments yielded similar results. **(d)** Distribution for $Nestin\text{-}GFP^{+}$ MSCs relative to central vain and bone (n=7 mice per group). **p*=0.0043 (t=3.62, df=120), ***p*=0.0299 (t=0.31, df=120) determined by two-way Anova Bonferroni's multiple comparisons test.**(e)** Frequency of compact bone (crushed bone) $CD45^{-}$ $Ter119^{-}$ $CD31^{-}$ $Nestin\text{-}GFP^{+}$ MSCs (n=3 mice per group). **(f)** CFU-F frequency of $CD45^{-}$ $Ter119^{-}$ $CD31^{-}$ $Nestin\text{-}GFP^{+}$ MSCs sorted from crushed bones and plated at equal numbers and clonal densities under CFU-F culture conditions (n=3 mice per group). Data represented as mean ± sem, *p* values determined by two-tailed *t*-test, unless indicated otherwise.

Supplementary Figure 2

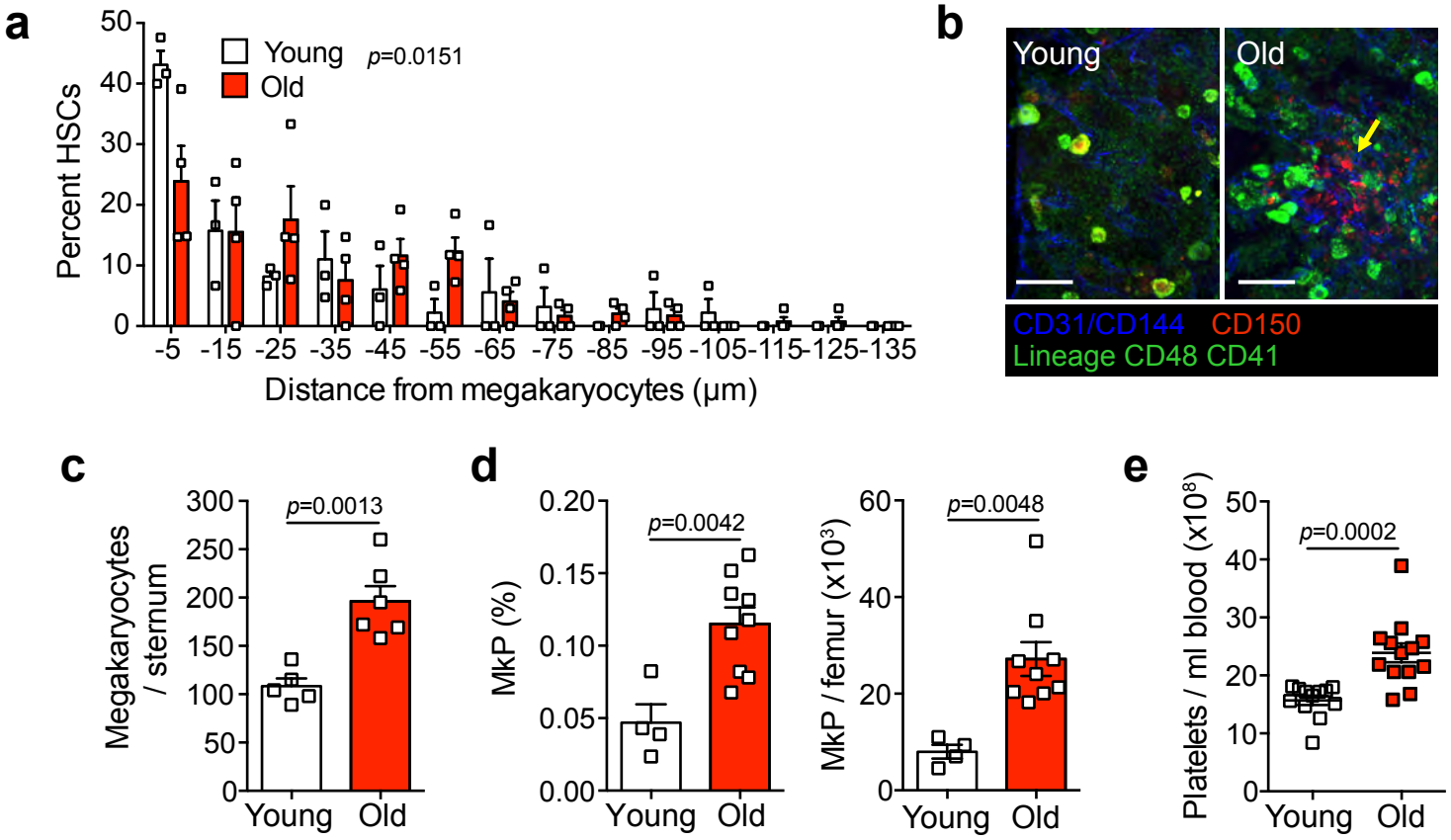

Supplementary Figure 2. Aging disrupts the megakaryocytic niche. **(a)** Distribution of HSCs in the sternal bone marrow relative to megakaryocytes (n = 47 young HSCs; 148 old HSCs 4; mice per group). Two-sample Kolmogorov-Smirnov test, *p*=0.0151. **(b)** Representative whole-mount confocal z-stack projections of sternal bone marrow from young and old C57BL/6 mice stained for $CD31^{+}/CD144^{+}$ double positive vasculature, lineage (CD3e, B220, Gr-1, Ter119, Mac-1), CD48, CD41 and CD150, Scale bar, 100 μm. Arrow denotes $CD150^{+}$ cell cluster. Three independent experiments yielded similar results. **(c, d, e)** Quantification of sternal megakaryocyte number (n=5 young, 6 old) **(c)**, absolute numbers of femur $lineage^{-}$ (B220, CD3e, Mac-1, Gr-1) $Sca\text{-}1^{+}$ $cKit^{+}$ $CD150^{+}$ $CD41^{+}$ megakaryocyte progenitors (MkP) (n=4 young, n=8 old) **(d)** and peripheral blood platelet counts (n=12 young, 13 old) **(e)** in young and old C57BL/6 mice. Data represented as mean ± sem, p value determined by two-tailed *t*-test, unless indicated otherwise.

Supplementary Figure 3

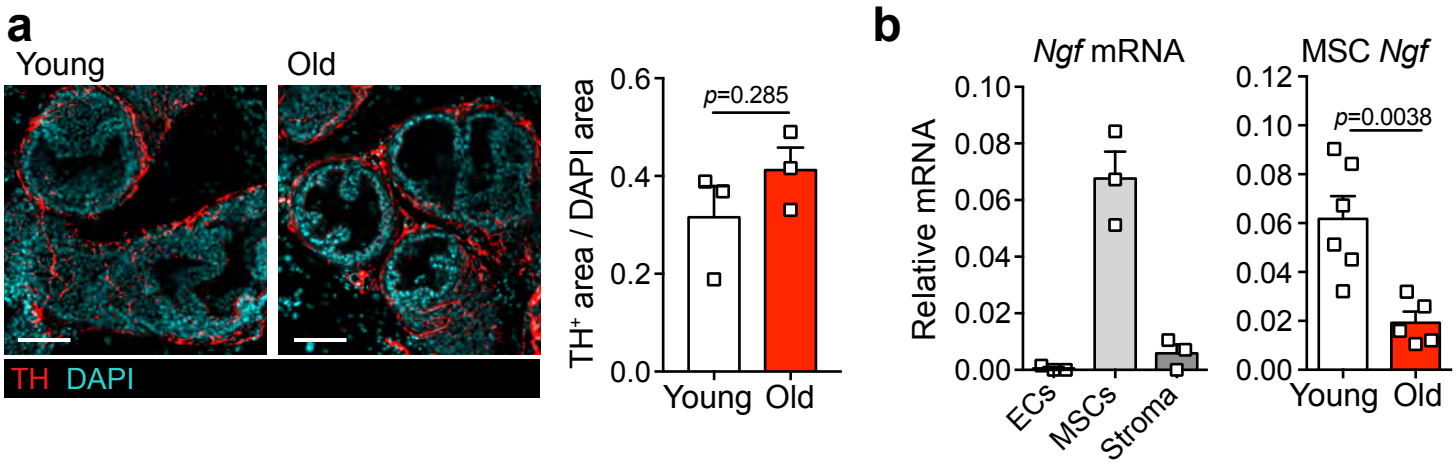

Supplementary Figure 3. Age associated SNS neuropathy is specific to the bone marrow.

(a) Left, confocal Z-stack montage projections of prostates from young and old C57BL/6 male mice stained for TH and DAPI. Scale bar, 100 μm. Right, quantification of TH covered prostate area relative to DAPI area (n=3 mice per group). **(b)** Left, quantification of *Ngf* mRNA levels in CD45$^-$ Ter119$^-$ CD31^{bright} Sca-1$^+$ ECs, CD45$^-$ Ter119$^-$ CD31$^-$ CD51$^+$ PDGFRα$^+$ MSCs and CD45$^-$ Ter119$^-$ CD31$^-$ CD51$^-$ PDGFRα$^-$ non-MSC stromal cells sorted from young mice (n=3 mice per group). Right, comparison of MSC *Ngf* mRNA levels sorted from young and old mice (n=6 young, 5 old). Data represented as mean ± sem, *p* value, determined by two-tailed *t*-test.

Supplementary Figure 4

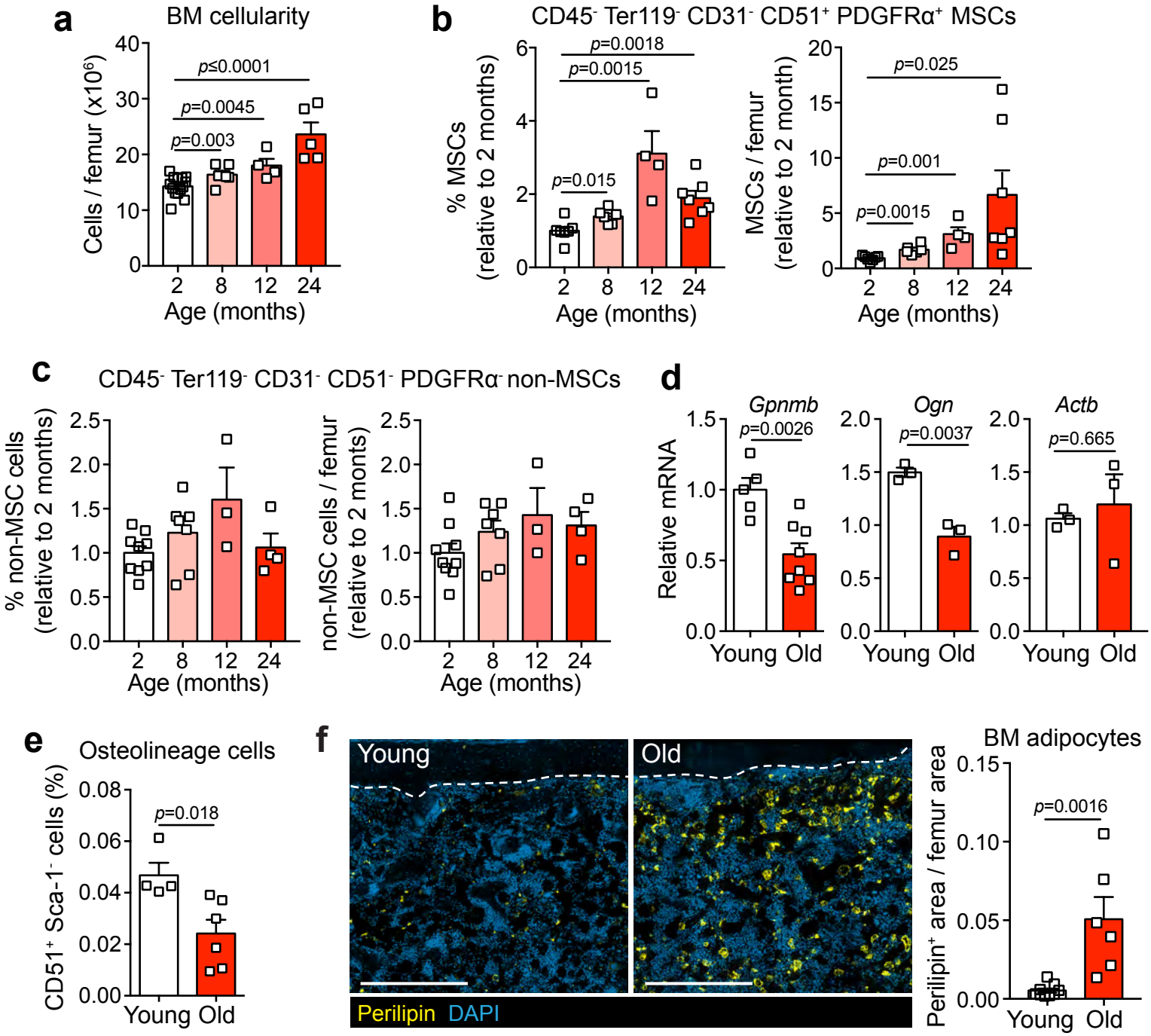

Supplementary Figure 4. Additional analyses of mesenchymal cells in aged HSC niche.

(a) Bone marrow cellularity at 2 (n=14), 8 (n=6), 12 (n=4) and 24 (n=5) months of age. **(b)** Absolute numbers and frequency of MSCs ($CD45^-$ $Ter119^-$ $CD31^-$ $CD51^+$ $PDGFR\alpha^+$) at 2 (n=7), 8 (n=6), 12 (n=4) and 24 (n=7) months of age. **(c)** Absolute numbers and frequency of non-MSC stromal cells ($CD45^-$ $Ter119^-$ $CD31^-$ $CD51^-$ $PDGFR\alpha^-$) at 2 (n=9), 8 (n=7), 12 (n=3) and 24 (n=4) months of age. **(d)** Quantification of mRNA levels of osteolineage genes *Gpnmb, Ogn* and *Actb* relative to *Gapdh* in sorted MSCs ($CD45^-$ $Ter119^-$ $CD31^-$ $CD51^+$ $PDGFR\alpha^+$) (*Gpnmb*: n=5 young, 8 old mice, *Ogn* and *Actb*: 3 mice per group). **(e)** Frequency of osteolineage cells ($CD45^-$ $Ter119^-$ $CD31^-$ $CD51^+$ $Sca\text{-}1^-$) derived from compact bone (n=4 young, 6 old mice). **(f)** Left, confocal z-stack projection montages of femurs stained for $CD31^+/CD144^+$ double positive vasculature, Perilipin and DAPI. Scale bar, 500 μm. Right, assessment of $perilipin^+$ cells by quantification of $perilipin^+$ area divided by total femur area (n=9 young, 6 old projections; 3 mice per group). Data represented as mean ± sem, *p* value determined by two-tailed *t*-test.

Supplementary Figure 5

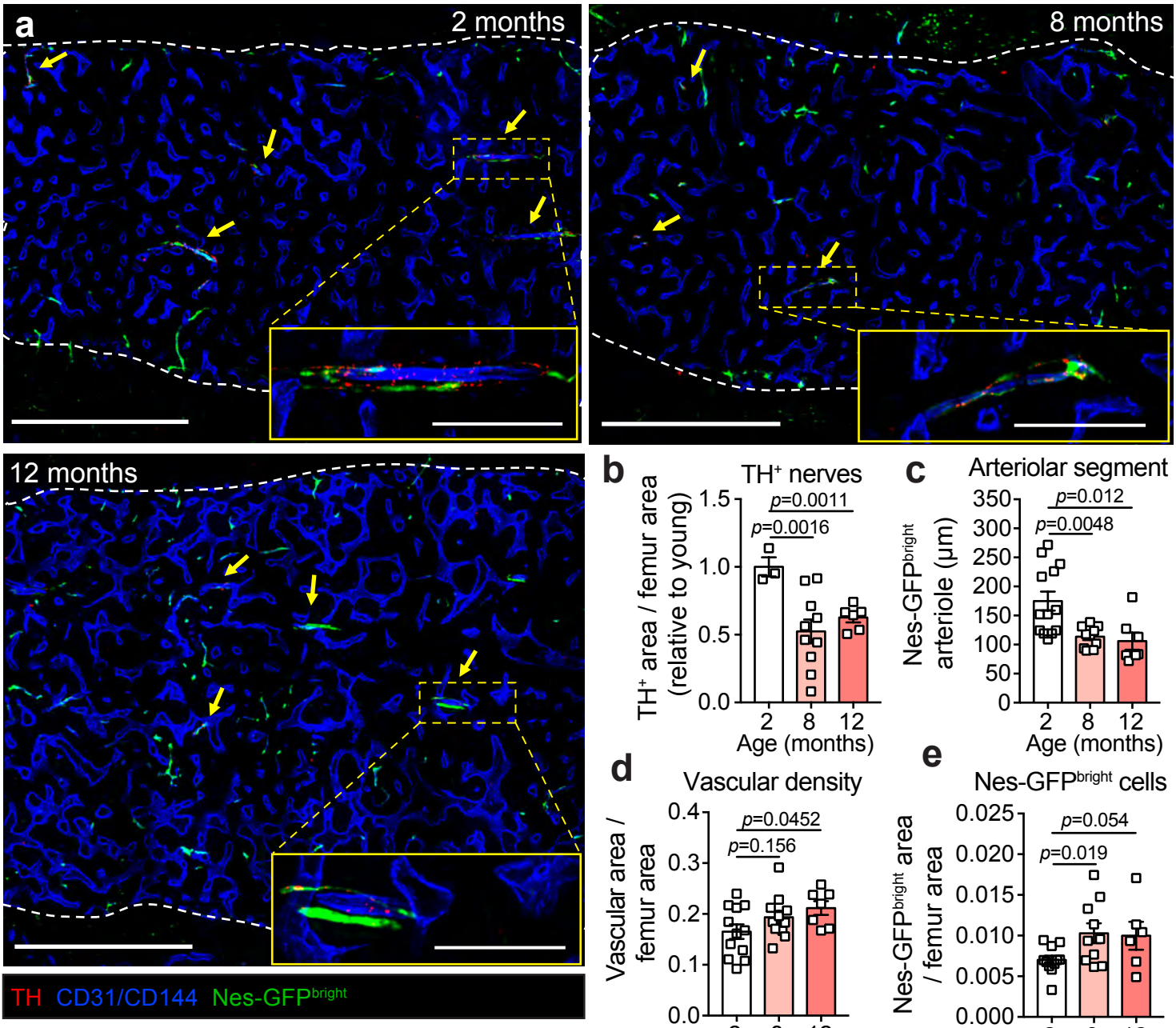

Supplementary Figure 5. Characterization of niche remodeling at different ages.

(a, b, c, d, e) Representative confocal z-stack projection montages from the bone marrow of 2, 8 and 12 month old *Nestin-GFP* mice stained for $CD31^+/CD144^+$ double positive vasculature and TH^+ nerves. Scale bar, 500 μm for femur montage and 100 μm for zoomed projections. Three independent experiments yielded similar results **(a)**, quantification of femur innervation, TH^+ area relative to femur area (n=3, 2 months, 11, 8 months and 5, 12 months projections; 3 mice per group) **(b)**, quantification of Nestin-GFP^{bright} arteriolar segment length (n=13, 2 months, 10, 8 months and 7, 12 months projections; 3 mice per group) **(c)**, vascular density, $CD31^+/CD144^+$ area relative to femur area (n=12, 2 months, 11, 8 months and 7, 12 months projections; 3 mice per group) **(d)** and quantification of Nestin-GFP^{bright} cells, Nestin-GFP^{bright} area relative to femur area (n=11, 2 months, 10, 8 months and 6, 12 months projections; 3 mice per group) **(e)** in femurs of 2, 8 and 12 month old *Nestin-GFP* mice. **(f)** Frequency and absolute numbers of HSCs (Lin^- $CD48^-$ $Sca\text{-}1^+$ $c\text{-}Kit^+$ $CD150^+$) in femurs of 2 (n=10), 8 (n=11), 12 (n=8), and 24 (n=4) month old C57BL/6 mice for frequency and 2 (n=12), 8 (n=8), 12 (n=4), and 24 (n=6) month old C57BL/6 mice for absolute numbers. **(g)** HSC distribution relative to Nestin-GFP^{bright} arterioles in 2, 8 and 12 month old *Nestin-GFP mice*. (n =181 HSCs at 2 months, 251 HSCs at 8 months, 321 HSCs at 12 months; 3 mice per age group). Two-sample Kolmogorov-Smirnov test $p \leq 0.0001$ for 8 month, $p \leq 0.0001$ for 12 month (each age group compared to 2 months old). Data represented as mean ± sem, *p* values determined by two-tailed *t*-test, unless indicated otherwise. For box plots, the box spans from the 25th to 75th percentiles and the centerline is plotted at the median. Whiskers represent minimum to maximum range.

Supplementary Figure 6

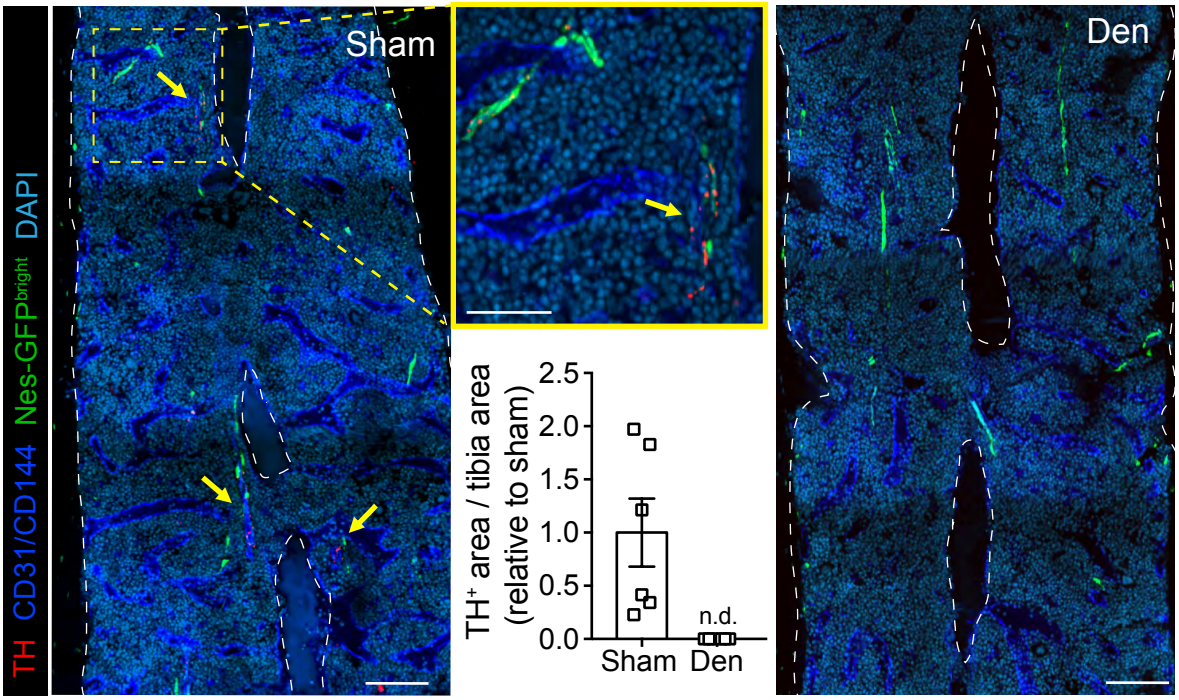

Supplementary Figure 6. Femoral and sciatic nerves denervation ablates SNS innervation of the bone marrow.

Representative confocal z-stack projection montages of sham and denervated tibiae from *Nestin-GFP* mice following denervation of sciatic and femoral nerves, stained for TH^+ nerves, $CD31^+/CD144^+$ double positive vasculature and DAPI, Scale bar, 500 μm for montage and 100 μm for zoomed projection. Bottom center, sympathetic innervation quantified by TH^+ area divided by total tibia area (n=6 projections from 4 mice per group). n.d. (not detected).

Supplementary Figure 7

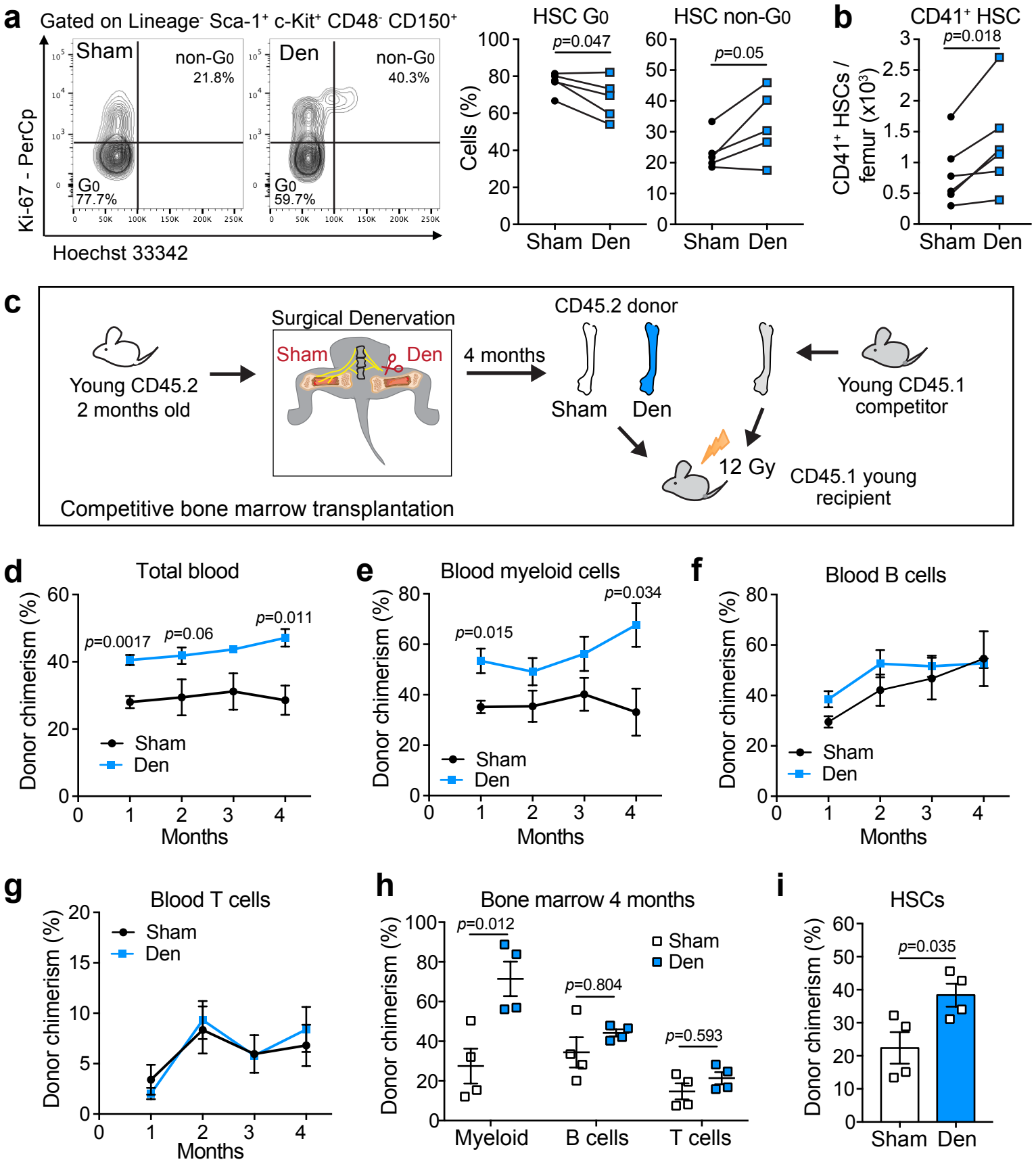

Supplementary Figure 7. Bone marrow denervation induces HSC aging phenotypes. **(a)** Left, representative FACS plots showing gating strategy for HSC Ki-67 and Hoechst 33342 staining. Right, quantification of HSC in G0 (Ki-67^{-}) and non-G0 (Ki-67^{+}) derived from sham and denervated femurs (n = 5 mice). **(b)** Absolute numbers of myeloid-biased CD41^{+} HSCs (lineage^{-} Sca-1^{+} c-Kit^{+} CD48^{-} CD150^{+} CD41^{+}) in sham and denervated femurs (n=5 mice). **(c)** Schematic illustration of bone marrow transplantation experiment following surgical denervation. **(d, e, f, g, h, i)** Total blood chimerism (CD45.2^{+}) **(d)**, blood myeloid cells chimerism (Mac-1^{+} CD45.2^{+}) **(e)**, blood B cells chimerism (B220^{+} CD45.2^{+}) **(f)**, blood T cells chimerism (CD4^{+}/CD8^{+} CD45.2^{+}) **(g),** 4 month bone marrow chimerism **(h)** and 4 month HSC chimerism **(i)** in CD45.1 recipient mice transplanted with whole bone marrow derived from either sham or denervated femurs in competition with equal numbers of young CD45.1 bone marrow cells (n= 4 sham, 4 denervated). Data represented as mean ± sem, *p* values determined by two-tailed paired *t*-test (**a**-**b**) and two-tailed unpaired *t*-test (**c**-**i**).

Supplementary Figure 8

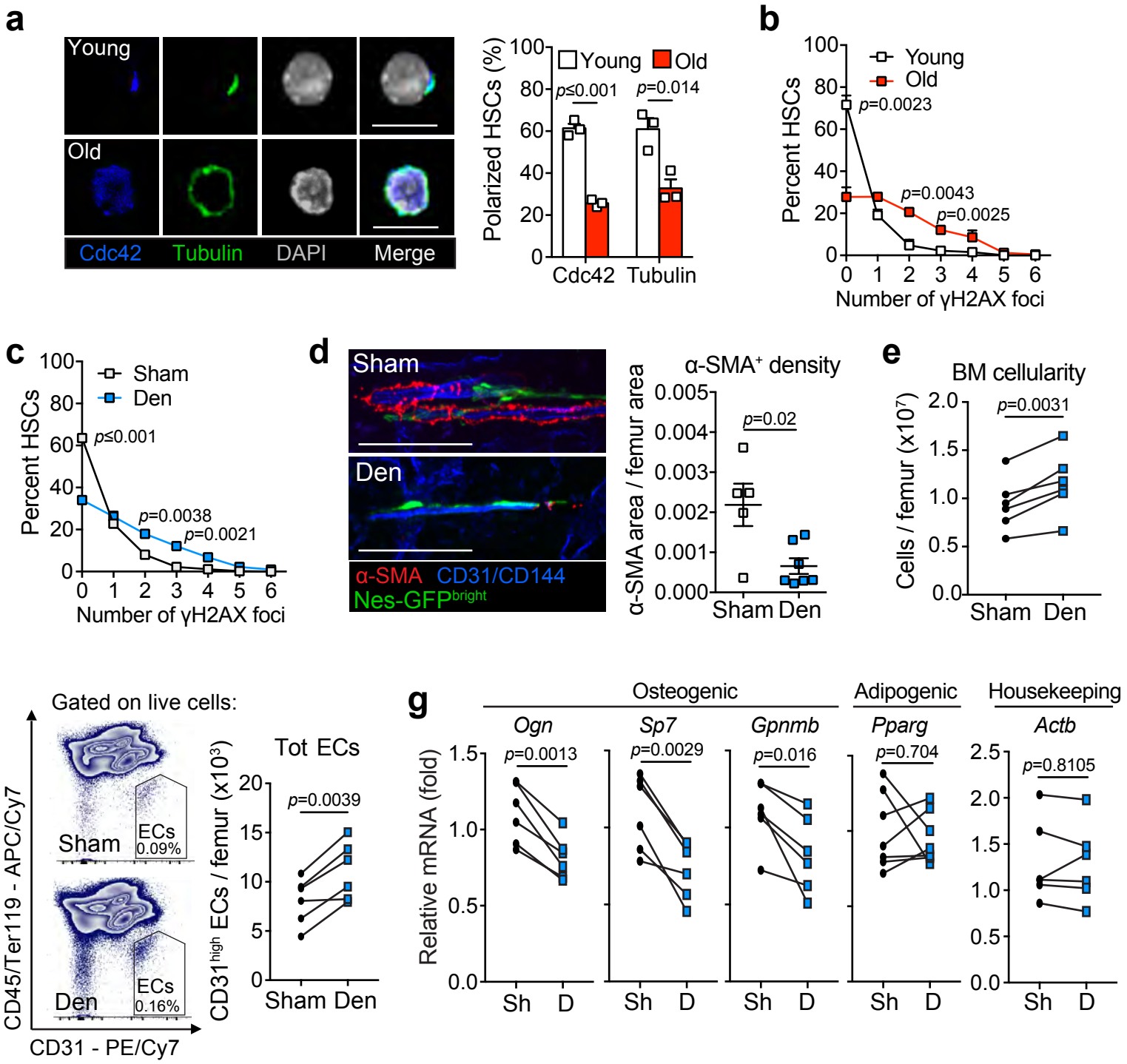

Supplementary Figure 8. HSC and niche characterization following bone marrow denervation.

(a) Left, representative confocal z-stack projections of HSCs sorted from young or old mice and stained with Cdc42, Tubulin and DAPI. Scale bar, 10 μm. Right, quantification of polarized HSCs (n calculated as mean of total 236 young and 331 old HSCs isolated from 3 mice per group). **(b, c)** Quantification of γH2AX foci in HSCs from data presented in Fig. 4f, comparing young and old HSCs **(b)** and sham and denervated HSCs **(c)**. **(d)** Left, representative z-stack confocal projections of sham and denervated tibiae stained with $CD31^+$/$CD144^+$ and α-SMA. Scale bar, 100 μm. Right, assessment of α-SMA^+ cells by quantification of α-SMA^+ area divided by total tibia area (n=5 sham, 7 denervated projections from 4 mice each). **(e)** BM cellularity in sham and denervated femurs of C57BL/6 young mice (n=6 mice). **(f)** Left, representative gating strategy for FACS quantification of total ECs ($CD45^-$ $Ter119^-$ $CD31^{bright}$). Right, absolute numbers of total ECs in femurs of sham and denervated mice (n=6 mice). **(g)** Quantification of osteogenic (*Ogn*, *Sp7* and *Gpnmb*), adipogenic (*Pparg*) and housekeeping (*Actb*) genes, mRNA relative to *Gapdh* in sorted MSCs ($CD45^-$ $Te119^-$ $CD31^-$ $CD51^+$ $PDGFR\alpha^+$) from sham (Sh) and denervated (D) femurs (n=6 mice). Data represented as mean ± s.e.m, *p* value determined by two-tailed unpaired *t*-test (**a**-**d**) and two-tailed paired *t*-test (**e**-**g**).

Supplementary Figure 9

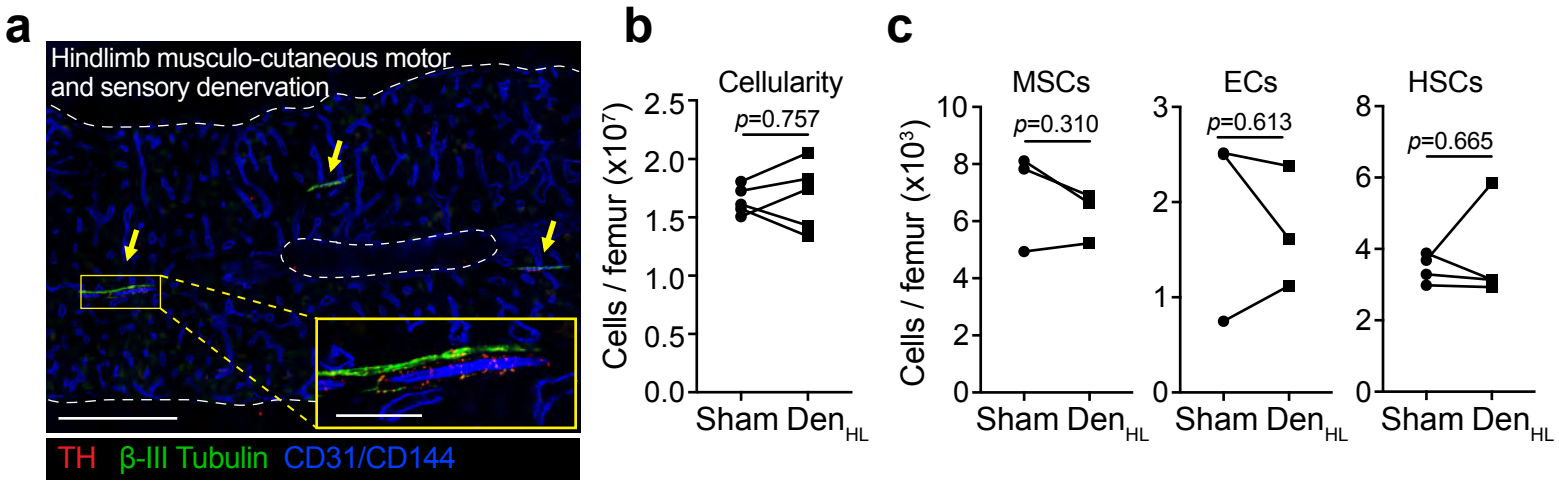

Supplementary Figure 9. Hindlimb musculo-cutaneous motor and sensory denervation does not affect the bone marrow.

(a) Representative confocal z-stack projection montage of denervated femurs, following musculo-cutaneous motor and sensory denervation, stained for $CD31^{+}/CD144^{+}$ double positive vasculature and TH and β-III Tubulin positive nerves. Scale bar, 500 μm. Arrows denote adrenergic nerves. **(b, c)** Bone marrow cellularity (n=5 mice) **(b)** and MSCs ($CD45^{-}$ $Ter119^{-}$ $CD31^{-}$ $CD51^{+}$ $PDGFR\alpha^{+}$), ECs ($CD45^{-}$ $Ter119^{-}$ $CD31^{bright}$) and HSCs ($lineage^{-}$ $Sca\text{-}1^{+}$ $c\text{-}Kit^{+}$ $CD48^{-}$ $CD150^{+}$) (n=3 mice) **(c)** 4 months after Hind limb denervation (Den_{HL}) compares to sham control. Data represented as mean ± s.e.m, *p* value determined by two-tailed paired *t*-test.

Supplementary Figure 10

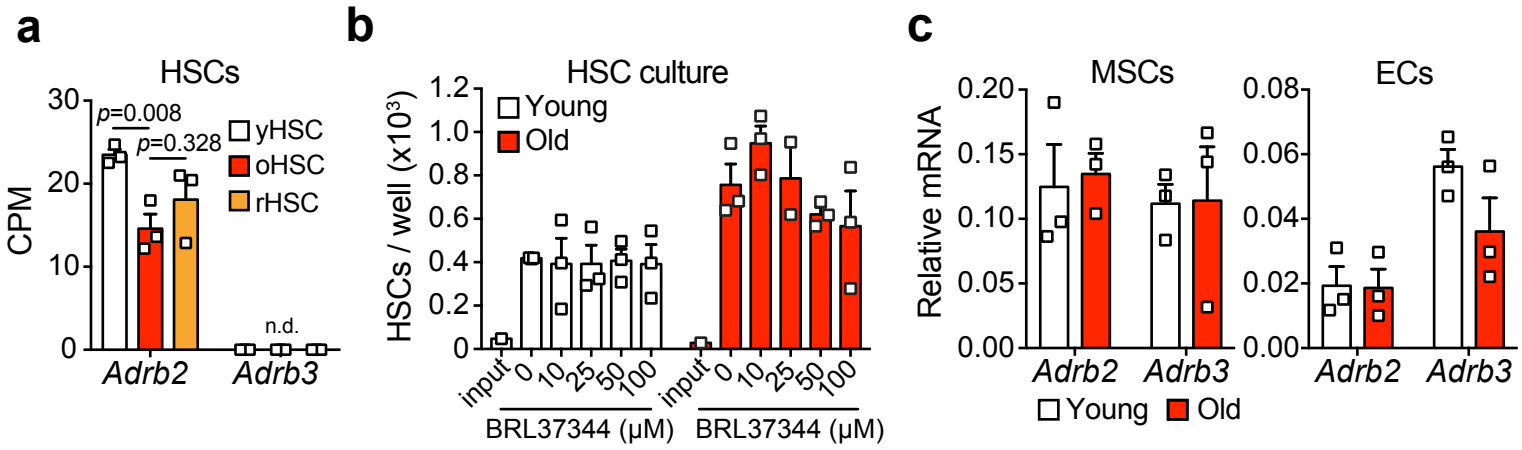

Supplementary Figure 10. Expression of *Adrb2* and *Adrb3* in HSCs, MSCs and ECs. **(a)** *Adrb2* and *Adrb3* transcript levels (CPM) in young HSCs (yHSCs), old HSCs (oHSCs) and BRL37344 rejuvenated HSCs (rHSCs) following RNA-seq analysis (n=3 mice per group). **(b)** *In vitro* culture of lineage$^-$ bone marrow in the presence of indicated concentration of BRL37344. HSCs numbers were quantified with FACS analysis after 5 day culture (n= 3 young, 3 old). **(c)** Quantification of mRNA levels of *Adrb2* and *Adrb3* relative to *Gapdh* in sorted MSCs (n=3 mice per group). Data represented as mean ± s.e.m. *p* value determined by two-tailed *t*-test. n.d. (not detected)

Supplementary Figure 11

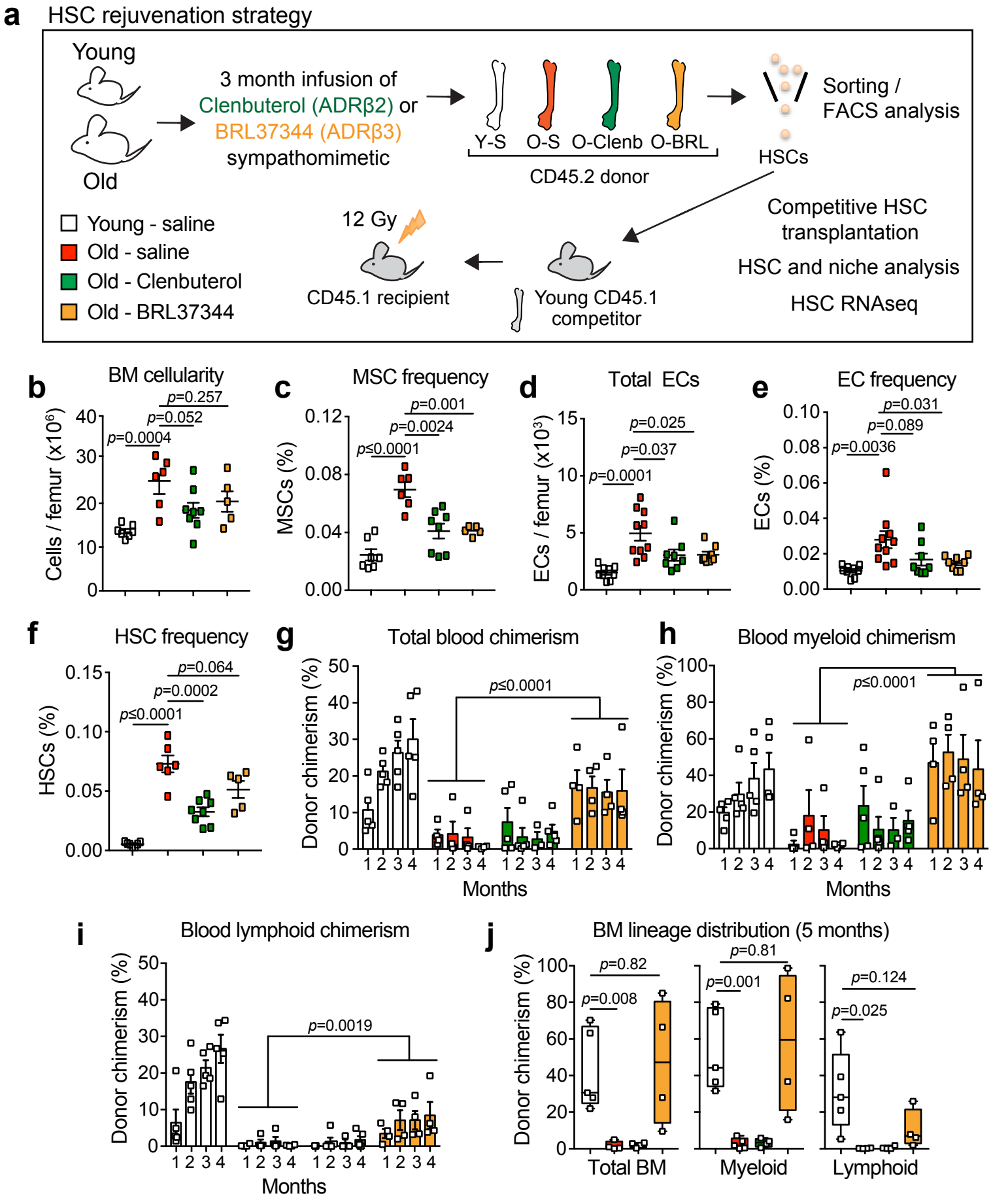

Supplementary Figure 11. Additional rejuvenation data following treatment with β-adrenergic agonists.

(a) Schematic illustration of experimental design for HSC rejuvenation with β-adrenergic-selective sympathomimetic. **(b, c, d, e, f)** Bone marrow cellularity (n=7 young-saline, 6 old-saline, 8 old-clenbuterol, 5 old-BRL37344) **(b)**, frequency of MSCs ($CD45^-$ $Te119^-$ $CD31^-$ $CD51^+$ $PDGFR\alpha^+$) (n=7 young-saline, 6 old-saline, 8 old-clenbuterol, 5 old-BRL37344) **(c)**, absolute numbers of total ECs ($CD45^-$ $Te119^-$ $CD31^{bright}$) (n=9 young-saline, 10 old-saline, 8 old-clenbuterol, 8 old-BRL37344) **(d)**, frequency of total ECs (n=9 young-saline, 10 old-saline, 8 old-clenbuterol, 8 old-BRL37344) **(e)** and frequency of HSCs (lin^- $CD48^-$ $Sca\text{-}1^+$ $c\text{-}Kit^+$ $CD150^+$) (n=7 young-saline, 6 o-saline, 8 old-clenbuterol, 5 old-BRL37344) **(f)** in young and old mice implanted with Alzet pumps with either saline, clenbuterol or BRL37344. **(g, h, i, j)** Total blood chimerism ($CD45.2^+$) **(g)**, blood myeloid cell chimerism ($Mac\text{-}1^+$ $CD45.2^+$) **(h)**, blood lymphoid cell chimerism ($B220^+$ $CD4^+$ $CD8^+$ $CD45.2^+$) **(i)** and bone marrow lineage distribution **(j)** 5 months after HSC transplantation (n=5 young-saline, 4 old-saline, 4 old-clenbuterol, 4 old-BRL37344). Data represented as mean ± s.e.m, *p* value determined by two-tailed unpaired *t*-test. For box plots, the box spans from the 25th to 75th percentiles and the centerline is plotted at the median. Whiskers represent minimum to maximum range

Supplementary Figure 12

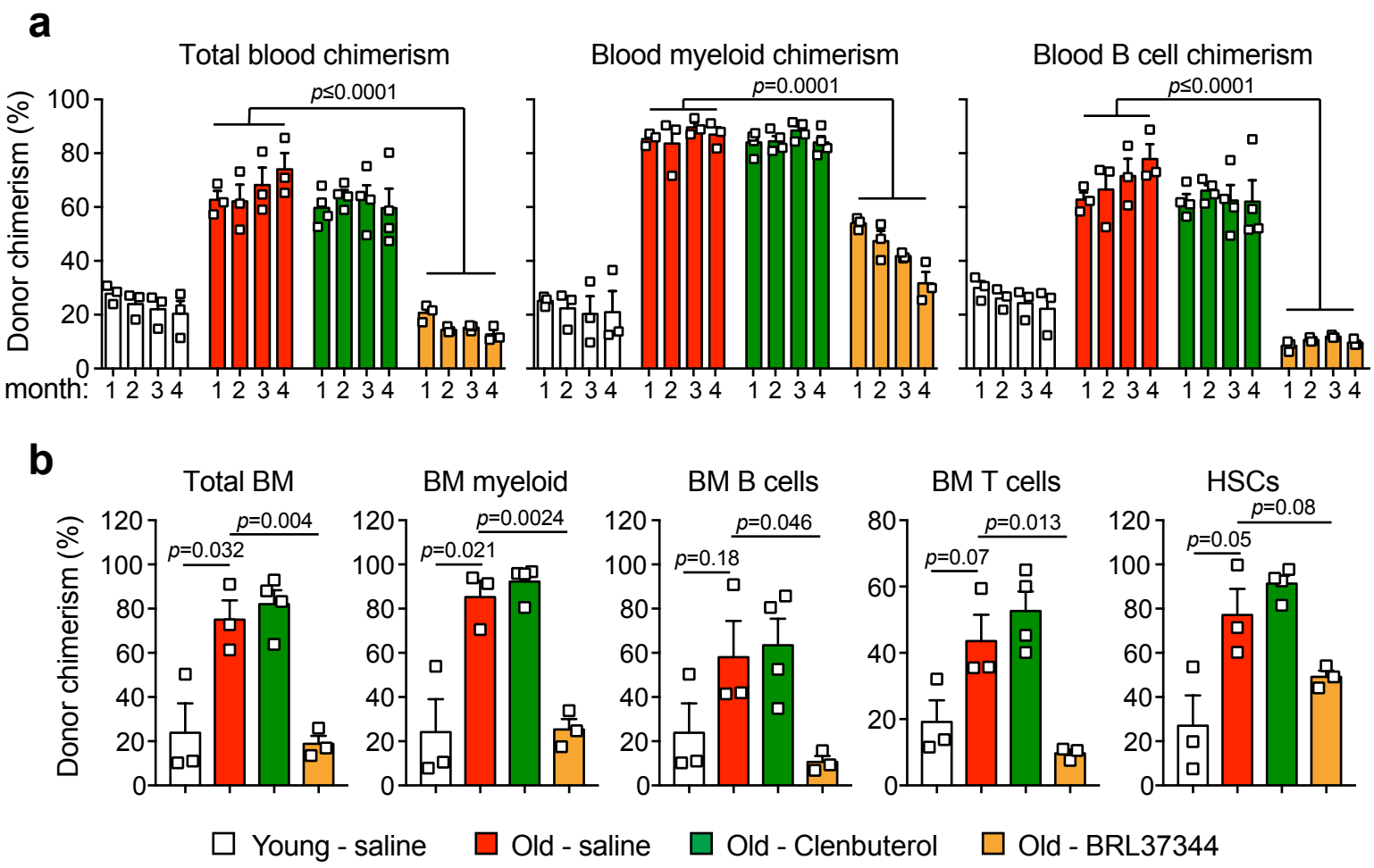

Supplementary Figure 12. Competitive bone marrow transplantation following rejuvenation with β-adrenergic agonists.

(a, b) Total blood chimerism ($CD45.2^+$), blood myeloid cell chimerism ($Mac\text{-}1^+$ $CD45.2^+$) and blood B cell chimerism ($B220^+$ $CD45.2^+$) **(a)**, 4 month total bone marrow chimerism**,** 4 month bone marrow myeloid cell chimerism, 4 month bone marrow B cell chimerism, 4 month bone marrow T cell chimerism ($CD4/CD8^+$ $CD45.2^+$) and 4 month HSC chimerism (lin^- $CD48^-$ $Sca\text{-}1^+$ $c\text{-}Kit^+$ $CD150^+$ $CD45.2^+$) **(b)** in CD45.1 recipient mice transplanted with bone marrow derived from β-adrenergic agonists treated mice in competition with equal numbers of young CD45.1 bone marrow competitior cells. (n= 3 young-saline, 3 old-saline, 4 old-clenbuterol and 3 old-BRL37344). Data represented as mean ± sem, *p* value determined by two-tailed *t*-test.

Supplementary Figure 13

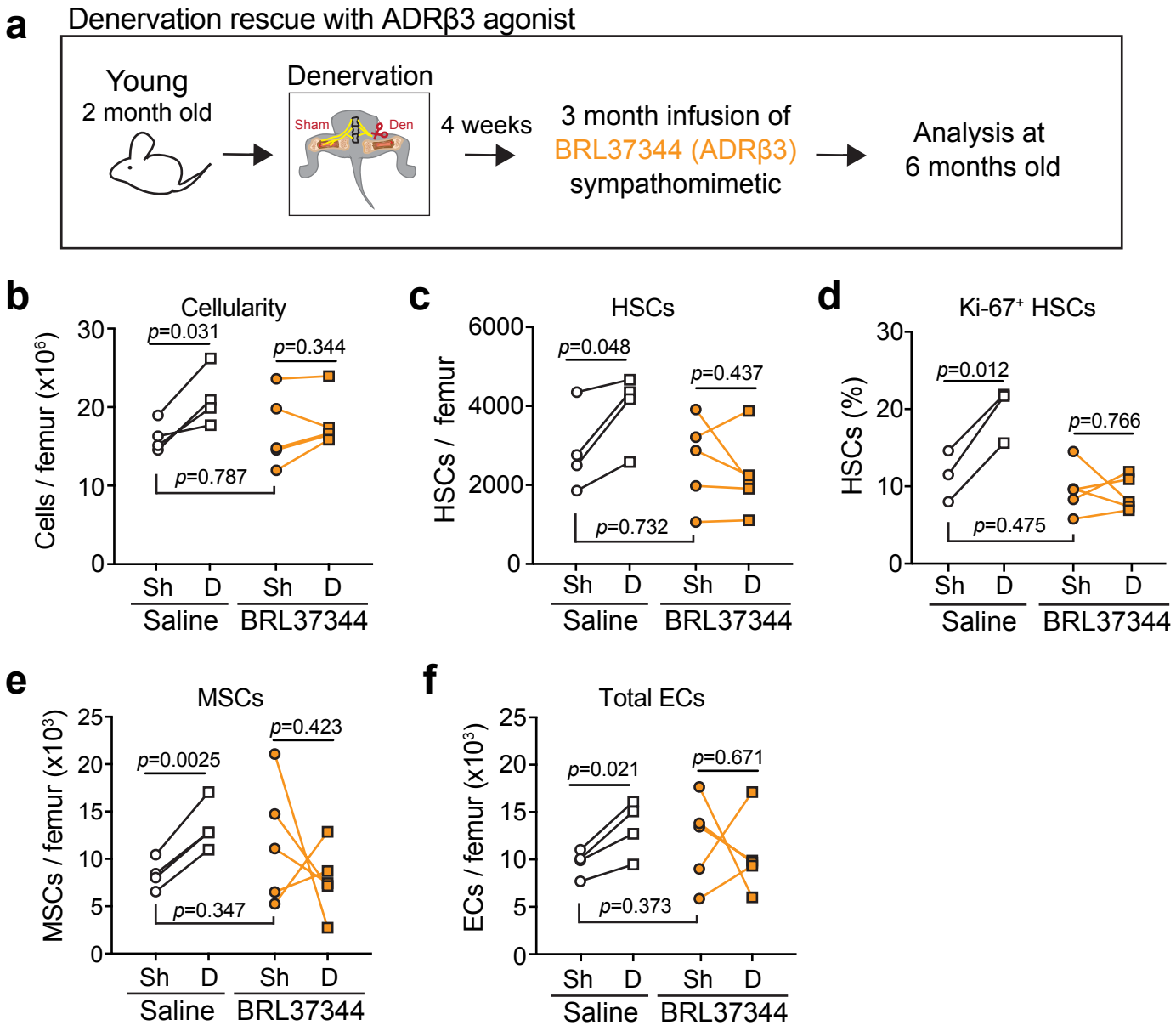

Supplementary Figure 13. β3-adrenergic agonist BRL37344 rescues the premature aging upon surgical denervation.

(a) Schematic illustration of experimental design for rescue of premature aging in denervated mice upon administration of ADRβ3 agonist BRL37344. **(b, c, d, e, f)** Bone marrow cellularity **(b)**, absolute numbers of HSCs (lin^- $CD48^-$ $Sca\text{-}1^+$ $c\text{-}Kit^+$ $CD150^+$)**(c)**, percentage of Ki-67^+ proliferating HSCs **(d)**, absolute numbers of MSCs ($CD45^-$ $Te119^-$ $CD31^-$ $CD51^+$ $PDGFR\alpha^+$) **(e)** and absolute numbers of total ECs ($CD45^-$ $Te119^-$ $CD31^{bright}$) **(f)** in denervated mice implanted with osmotic pumps containing either BRL37344 or saline as control (n=4 saline, 5 BRL37344 mice). Data represented as mean ± s.e.m, *p* value determined by two-tailed paired *t*-test, comparing Sham (Sh) and Denervated (D) within the same mouse, and two-tailed unpaired *t*-test, comparing sham groups between different mice.

Supplementary Figure 14

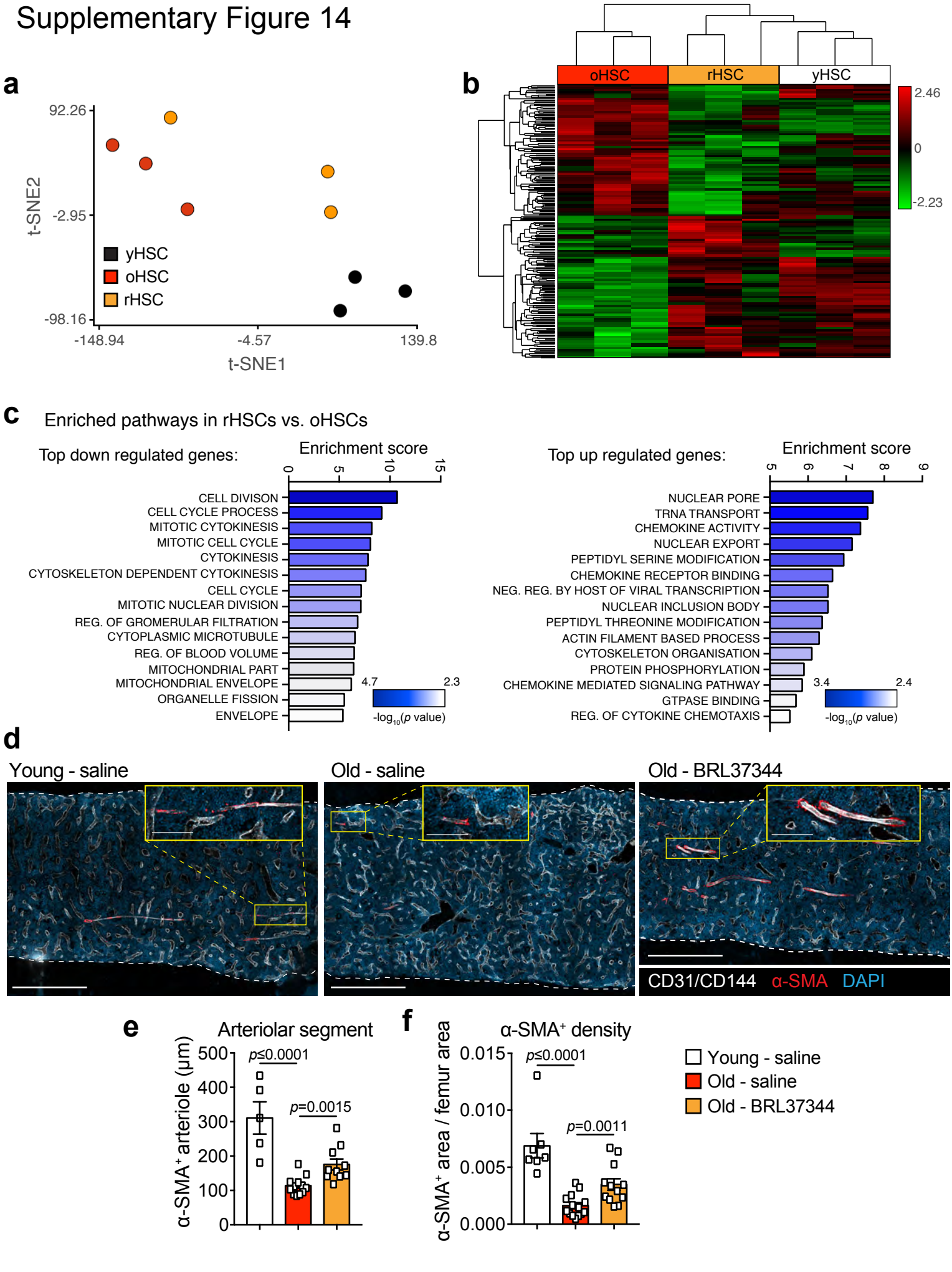

Supplementary Figure 14. Rejuvenation of HSCs and niche following β3-adrenergic agonist BRL37344 treatment of old mice.

(a) t-SNE plot depicting distribution of young HSCs (yHSCs), old HSCs (oHSCs) and BRL37344-rejuvenated HSCs (rHSCs) following RNA-seq analysis. **(b)** Unsupervised hierarchical clustering of top variable genes, comparing oHSCs and rHSCs. **(c)** Enriched pathways of top up regulated and down regulated genes in rHSCs compared to oHSCs (n=3 samples per group). The enrichment score was calculated as the negative natural logarithm of the enriched *p* value derived from Fisher's exact test. **(d)** Representative confocal z-stack projection montages of femurs from young (2 months) and old (15-20 months) C57BL/6 mice treated with either saline or BRL37344 for 12 weeks and stained for $CD31^+$/ $CD144^+$ double positive vasculature, α-SMA^+ cells and DAPI. Scale bars, 500 μm for montage, and 100 μm for zoomed projection. Three independent experiments yielded similar results. **(e)** Assessment of arteriolar segment length by measuring the length of α-SMA signal covering $CD31^+$/$CD144^+$ arterioles in femurs of mice described in (**d**) (n=5 young-saline, 12 old-saline, 10 old-BRL37344 projections; 3 mice per group). **(f)** Assessment of α-SMA^+ cell density by quantification of α-SMA^+ area divided by total femur area (n=6 young-saline, 13 old-saline, 12 old-BRL37344 projections; 3 mice per group). Data represented as mean ± s.e.m. *p* value determined by two-tailed *t*-test.

Supplementary Figure 15

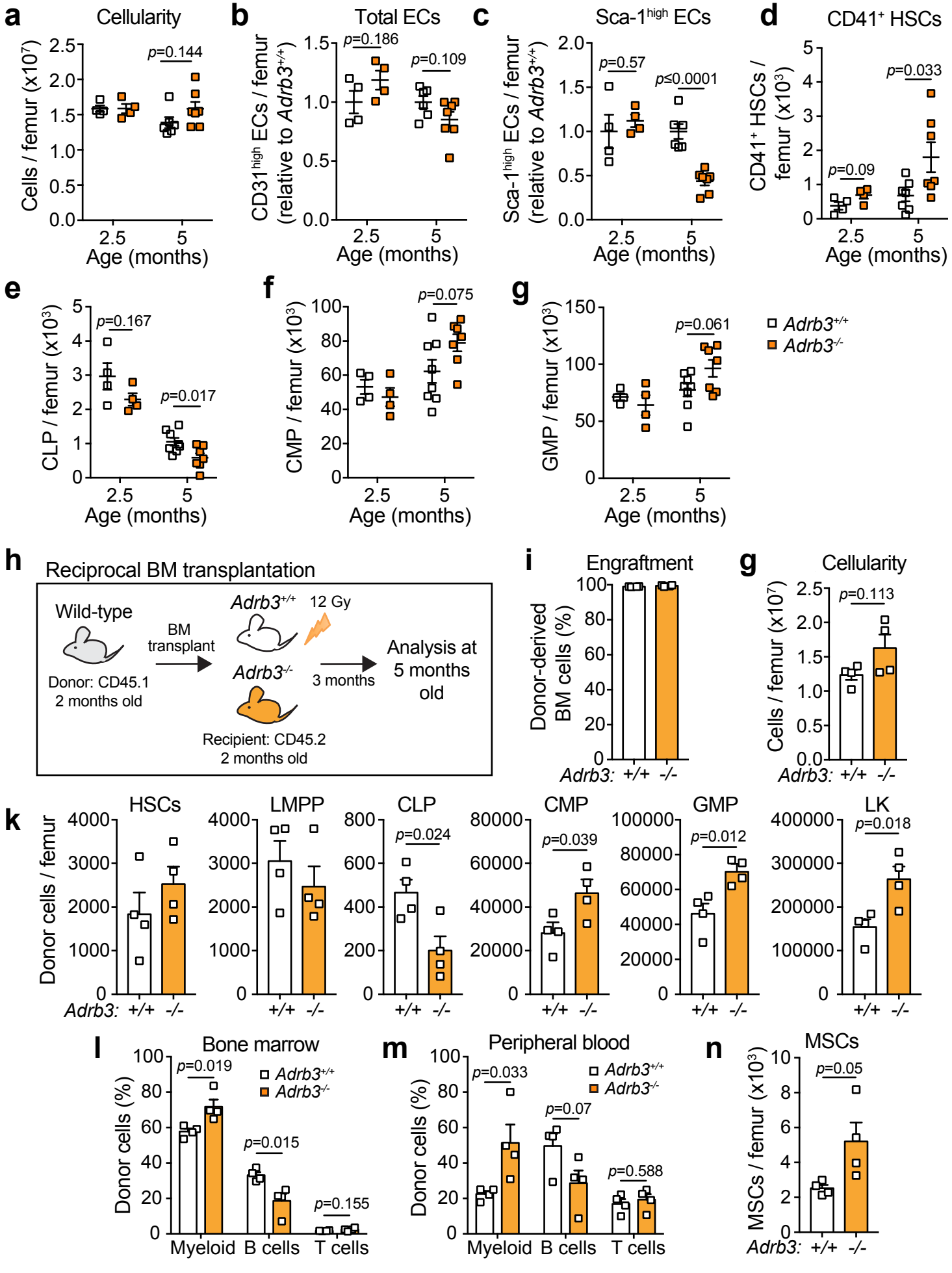

Supplementary Figure 15. Niche-derived ADRβ3 signals regulate HSC aging. (a, b, c, d, e, f, g) Bone marrow cellularity **(a)**, absolute numbers of total ECs ($CD45^-$ $Te119^-$ $CD31^{bright}$) **(b)**, absolute numbers of arteriolar ECs ($CD45^-$ $Te119^-$ $CD31^{bright}$ $Sca\text{-}1^{bright}$) (2.5 months: n=4 $Adrb3^{+/+}$, 4 $Adrb3^{-/-}$ and 5 months: n=6 $Adrb3^{+/+}$, 7 $Adrb3^{-/-}$) **(c),** absolute numbers of $CD41^+$ HSCs (lin^- $CD48^-$ $Sca\text{-}1^+$ $c\text{-}Kit^+$ $CD150^+$ $CD41^+$) (2.5 months: n=4 $Adrb3^{+/+}$, 4 $Adrb3^{-/-}$ and 5 months: n=7 $Adrb3^{+/+}$, 7 $Adrb3^{-/-}$) **(d),** absolute numbers of CLPs (lin^- $Sca\text{-}1^{low}$ $c\text{-}Kit^{low}$ $IL7R\alpha^+$ $Flt3^+$) **(e)**, absolute number of CMPs (lin^- $Sca\text{-}1^-$ $c\text{-}Kit^+$ $Fc\gamma R^{low}$ $CD34^+$) **(f)** and absolute number of GMPs (lin^- $Sca\text{-}1^-$ $c\text{-}Kit^+$ $Fc\gamma R^+$ $CD34^+$) **(g)** (2.5 months: n=4 $Adrb3^{+/+}$, 4 $Adrb3^{-/-}$ and 5 months: n=8 $Adrb3^{+/+}$, 7 $Adrb3^{-/-}$) in femurs of 2.5 and 5 months old $Adrb3^{+/+}$ and $Adrb3^{-/-}$ mice. **(h)** Schematic illustration of experimental design for reciprocal bone marrow transplantation of wild-type bone marrow into $Adrb3^{+/+}$ and $Adrb3^{-/-}$ mice. **(i)** Donor-derived CD45.1 cells 3 months after reciprocal transplantation. **(g)** Bone marrow cellularity of mice described in (**h**). **(k)** Absolute numbers of donor HSCs, LMPPs ($lineage^-$ $Sca\text{-}1^+$ $c\text{-}Kit^+$ $CD34^+$ $Flt3^+$), CLPs, CMPs, GMPs and LK progenitors ($lineage^-$ $Sca\text{-}1^-$ $c\text{-}Kit^+$) in femurs of mice described in (**h**). **(l, m)** Bone marrow **(l)** and blood **(m)** donor myeloid cells ($Mac\text{-}1^+$), B cells ($B220^+$) and T cells ($CD4^+$ $CD8^+$) in mice described in (**h**). **(n)** Absolute numbers of recipient MSCs ($CD45^-$ $Te119^-$ $CD31^-$ $CD51^+$ $PDGFR\alpha^+$) in mice described in (**h**). Data represented as mean ± sem, *p* value determined by two-tailed *t*-test. (n=4 mice per group for **i**-**n**)

Supplementary Table 1. Blood counts in β-adrenergic agonist-treated mice.

	WBC $x10^3/\mu l$	RBC $x10^6/\mu l$	HGB g/dL	HCT %	MCV fL	PLT $x10^3/\mu l$
Young Saline	6.5 ± 0.7	10.1 ± 0.2	13.3 ± 0.3	48 ± 1	474 ± 5	1,555 ± 33
Old Saline	6.7 ± 0.7	9.7 ± 0.3	12.3 ± 0.3	45 ± 1	397 ± 8	2,425 ± 283
Old BRL37344	6.5 ± 0.9	9.6 ± 0.3	12.6 ± 0.5	45 ± 1	472 ± 8	2,176 ± 103
Old Clenbuterol	6.3 ± 0.8	8.9 ± 0.8	11.3 ± 0.8	42 ± 3	486 ± 3	1,791 ± 188
P* value	0.84	0.2	0.03	0.08	0.35	0.022
P* value*	0.9	0.85	0.54	0.96	0.24	0.36
P* value**	0.78	0.45	0.41	0.33	0.233	0.087

Peripheral blood counts (CBC) of saline (n=4 young mice, n=4 old mice), Clenbuterol (n=6) and BRL37344 (n=6) treated mice. Blood was collected 12 weeks following pump implantation. WBC: white blood cells; RBC: red blood cells; HGB: hemoglobin; HCT: haematocrit; MCV: mean cell volume; PLT: platelets. Data represented as mean ± s.e.m. * Student *t*-test comparing young mice treated with saline and old mice treated with saline. ** Student *t*-test comparing old mice treated with saline and old mice treated with BRL37344. *** Student *t*-test comparing old mice treated with saline and old mice treated with Clenbuterol.